Supplementary Document to *Realized Illiquidity*

Demetrio Lacava [*] Angelo Ranaldo[†] Paolo Santucci de Magistris [‡]

March 18, 2026

[*]University of Messina, Department of Economics, Via dei Verdi, 98122 Messina, Italy. dlacava@unime.it. ORCID: https://orcid.org/0000-0002-9622-2120

[†]University of Basel and Swiss Finance Institute, Switzerland. angelo.ranaldo@unibas.ch. https://ORCID: 0000-0002-8785-816X

[‡]Luiss University, Department of Economics and Financial Markets, Viale Romania 32, 00197 Roma, Italy; sdemagistris@luiss.it. ORCID: https://orcid.org/0000-0002-6526-4803

1 Monte Carlo simulations

1.1 Constant volatility

We assess the quality of the measurement of illiquidity based on the realized Amihud by Monte Carlo simulations, in which the daily horizon is taken as the reference unit interval. The liquidity process, $\ell(t)$, is generated according to a Ornstein–Uhlenbeck process on $\log \ell(t)$, similar to the one used in Melino and Turnbull (1990) and Comte and Renault (1998) in the stochastic volatility context,

$$d \log \ell(t) = \kappa_\ell(\log \ell(t) - \ell_0)dt + \eta_\ell dW_\ell(t), \quad t > 0, \tag{1}$$

where $\exp(\ell_0) = 1$ represents the long-term mean. We then rescale $\ell(t)$ by a factor $\bar{\ell} = 10e03, 10e06, 10e10$ to indicate low-, medium-, and high-liquidity scenarios, respectively. The parameters κ_ℓ and η_ℓ determine the speed of the mean-reversion and the volatility of liquidity, respectively. In line with the empirical evidence displayed in the main document, the simulated liquidity process $\ell(t)$ also displays a persistent behavior. The reservation prices (and, hence, equilibrium prices) are generated according to the diffusive process in with $J = 2$. The variance coefficients are set to $\sigma_1^2 = 2.2$ and $\sigma_2^2 = 2.2$, respectively, while $\mu_j = 0$. This generates a daily standard deviation of log-returns of roughly 1.5%. In the simulation of price and volume trajectories, we consider $M = 1,000$ Monte Carlo replications for $T = 1,000$ transaction days and $I^* = 5,760$ intra-daily intervals corresponding to a 15-second frequency over 24 hours. RPV is then computed aggregating at daily horizon the absolute returns sampled at different frequencies: 1 hour; 30, 15, 10, 5 minutes; and 30 and 15 seconds, that is $I = [24, 48, 96, 144, 288, 1440, 2880, 5760]$ equally-spaced sub-intervals, respectively. Trading volume is obtained aggregating at daily horizon the volume generated in each sub-period. Hence, for each Monte Carlo simulation and for each sampling frequency, we obtain a time-series of realized Amihud $\{\mathcal{A}_t\}_{t=1}^T$ that we compare with the simulated time-series of integrated illiquidity, $\{\frac{1}{\mathcal{L}_t^*}\}_{t=1}^T$, where $\mathcal{L}_t^* = \sum_{i=1}^{I^*} \ell_{i,t}$, $t = 1, \ldots, T$.

1.1.1 Baseline Setting

The summary of the results of the baseline Monte Carlo simulations are presented in Table 1. In the baseline setting, the parameters of illiquidity (κ_ℓ and η_ℓ) are calibrated by indirect inference on the time series of realized Amihud of the DJ30 index, following the approach outlined in Corsi and Renò (2012) and Rossi and Santucci de Magistris (2018). The level of illiquidity, $\bar{\ell}$, is calibrated to the scale of the sample average of daily $\mathcal{A}$ of the DJ30 index.

From Table 1, it emerges that realized Amihud provides accurate measurements of the true integrated illiquidity process (i.e., $\frac{1}{\mathcal{L}}$) in all scenarios (low-, medium-, and high-illiquidity levels) with a bias (relative to the illiquidity signal) below 0.5% in absolute value and a small RMSE, even for relatively moderate sampling frequencies (e.g., 5-10 minutes). As expected from Proposition 1, the RMSE decreases as I increases (i.e., δ decreases). In general the RMSE of the realized Amihud is much smaller compared with the RMSE achieved by the daily Amihud. This result confirms that the classic daily Amihud represents the limiting case of an illiquidity measurement obtained with only one observation per trading period, that is, $I = \delta = 1$. In this case, the illiquidity measure reduces to $\mathcal{A}^D = \frac{|r|}{v}$.

A number of alternative parametric settings for the Monte Carlo have been considered and the results are reported in the sections below.

Low Liquidity						
	Percentage Relative Bias		Relative RMSE		Relative RMAE	
Sampling frequency	$\mathcal{A}$	$\mathcal{A}^D$	$\mathcal{A}$	$\mathcal{A}^D$	$\mathcal{A}$	$\mathcal{A}^D$
1h	2.5064	2.5255	0.2367	0.8271	0.1780	0.6310
30min	1.3053	1.3135	0.1615	0.7999	0.1236	0.6194
15min	0.4249	0.5965	0.1116	0.7866	0.0868	0.6126
10min	0.5068	0.6544	0.0914	0.7879	0.0713	0.6132
5min	0.3320	0.3986	0.0645	0.7837	0.0505	0.6102
1min	0.0117	0.1459	0.0291	0.7805	0.0226	0.6087
30sec	0.0024	0.1237	0.0203	0.7799	0.0158	0.6086
15sec	0.0104	0.1431	**0.0145**	0.7798	0.0113	0.6087
Medium Liquidity						
	Percentage Relative Bias		Relative RMSE		Relative RMAE	
Sampling frequency	$\mathcal{A}$	$\mathcal{A}^D$	$\mathcal{A}$	$\mathcal{A}^D$	$\mathcal{A}$	$\mathcal{A}^D$
1h	2.4313	3.0904	0.2381	0.8289	0.1798	0.6275
30min	1.3622	2.0892	0.1628	0.8005	0.1249	0.6164
15min	0.7243	1.2423	0.1122	0.7839	0.0869	0.6087
10min	0.4585	1.0875	0.0918	0.7815	0.0710	0.6082
5min	0.2705	0.9411	0.0643	0.7788	0.0500	0.6064
1min	0.0027	0.7611	0.0286	0.7752	0.0222	0.6051
30sec	-0.0010	0.7505	0.0201	0.7749	0.0157	0.6050
15sec	-0.0356	0.7269	**0.0145**	0.7751	0.0113	0.6048
High Liquidity						
	Percentage Relative Bias		Relative RMSE		Relative RMAE	
Sampling frequency	$\mathcal{A}$	$\mathcal{A}^D$	$\mathcal{A}$	$\mathcal{A}^D$	$\mathcal{A}$	$\mathcal{A}^D$
1h	2.5047	2.9398	0.2364	0.8270	0.1797	0.6344
30min	1.0042	1.3463	0.1614	0.7984	0.1247	0.6214
15min	0.4001	0.6476	0.1125	0.7858	0.0872	0.6154
10min	0.2307	0.6025	0.0925	0.7851	0.0722	0.6148
5min	0.2087	0.5966	0.0648	0.7834	0.0506	0.6143
1min	0.0338	0.3165	0.0292	0.7781	0.0226	0.6111
30sec	0.0083	0.2773	0.0206	0.7774	0.0160	0.6110
15sec	-0.0035	0.2641	**0.0143**	0.7771	0.0112	0.6108

Table 1: Illiquidity measurement. The table reports the Monte Carlo relative percentage bias, RMSE and, RMAE (all relative to $\frac{1}{\mathcal{L}}$) for several illiquidity estimators: the realized Amihud $\mathcal{A} = \frac{RPV}{v}$; the daily Amihud measure, that is, $\mathcal{A}^D = \frac{|r|}{v}$. The series $\ell(t)$ is generated according to the log Ornstein–Uhlenbeck process in (1), with parameters $\kappa_\ell = 0.4$ and $\eta_\ell = 0.8$. The smallest RMSE is in bold.

1.1.2 Setting 1

Low Liquidity						
	Percentage Relative Bias		Relative RMSE		Relative RMAE	
Sampling frequency	$\mathcal{A}$	$\mathcal{A}^D$	$\mathcal{A}$	$\mathcal{A}^D$	$\mathcal{A}$	$\mathcal{A}^D$
1h	2.5709	2.4434	0.2488	0.8633	0.1796	0.6325
30min	1.3537	1.1948	0.1694	0.8321	0.1245	0.6202
15min	0.4403	0.4113	0.1166	0.8167	0.0873	0.6130
10min	0.5363	0.4958	0.0957	0.8193	0.0717	0.6137
5min	0.3300	0.2339	0.0674	0.8152	0.0507	0.6108
1min	0.0078	-0.0120	0.0304	0.8123	0.0228	0.6094
30sec	-0.0021	-0.0377	0.0211	0.8116	0.0159	0.6093
15sec	0.0075	-0.0207	**0.0152**	0.8113	0.0114	0.6093
Medium Liquidity						
	Percentage Relative Bias		Relative RMSE		Relative RMAE	
Sampling frequency	$\mathcal{A}$	$\mathcal{A}^D$	$\mathcal{A}$	$\mathcal{A}^D$	$\mathcal{A}$	$\mathcal{A}^D$
1h	2.5680	3.2298	0.2499	0.8654	0.1815	0.6285
30min	1.3982	2.1673	0.1710	0.8360	0.1259	0.6174
15min	0.7458	1.2701	0.1173	0.8162	0.0875	0.6092
10min	0.4570	1.0957	0.0963	0.8130	0.0714	0.6086
5min	0.2640	0.9486	0.0673	0.8104	0.0503	0.6067
1min	-0.0006	0.7726	0.0299	0.8065	0.0223	0.6055
30sec	-0.0058	0.7598	0.0210	0.8064	0.0158	0.6054
15sec	-0.0390	0.7384	**0.0151**	0.8068	0.0113	0.6053
High Liquidity						
	Percentage Relative Bias		Relative RMSE		Relative RMAE	
Sampling frequency	$\mathcal{A}$	$\mathcal{A}^D$	$\mathcal{A}$	$\mathcal{A}^D$	$\mathcal{A}$	$\mathcal{A}^D$
1h	2.5574	2.8721	0.2464	0.8599	0.1802	0.6340
30min	1.0367	1.2020	0.1679	0.8268	0.1252	0.6201
15min	0.3955	0.4729	0.1173	0.8127	0.0876	0.6140
10min	0.2488	0.4526	0.0967	0.8130	0.0725	0.6137
5min	0.2087	0.4293	0.0681	0.8110	0.0509	0.6129
1min	0.0409	0.1554	0.0307	0.8056	0.0228	0.6098
30sec	0.0097	0.1111	0.0216	0.8047	0.0161	0.6096
15sec	-0.0041	0.0969	**0.0149**	0.8043	0.0112	0.6094

Table 2: Illiquidity measurement. The table reports the Monte Carlo relative percentage bias, RMSE and, RMAE (all relative to $\frac{1}{\mathcal{L}}$) for several illiquidity estimators: the realized Amihud $\mathcal{A} = \frac{RPV}{v}$; the daily Amihud measure, that is, $\mathcal{A}^D = \frac{|r|}{v}$. The series $\ell(t)$ is generated according to the log Ornstein–Uhlenbeck process in (1), with parameters $\kappa_\ell = 0.6$ and $\eta_\ell = 0.4$. The smallest RMSE is in bold.

1.1.3 Setting 2

Low Liquidity						
	Percentage Relative Bias		Relative RMSE		Relative RMAE	
Sampling frequency	$\mathcal{A}$	$\mathcal{A}^D$	$\mathcal{A}$	$\mathcal{A}^D$	$\mathcal{A}$	$\mathcal{A}^D$
1h	2.5735	3.0485	0.2440	0.8583	0.1776	0.6324
30min	1.3010	1.8125	0.1660	0.8302	0.1233	0.6209
15min	0.4184	1.0835	0.1146	0.8173	0.0866	0.6143
10min	0.4737	1.1342	0.0936	0.8179	0.0711	0.6148
5min	0.3206	0.9119	0.0663	0.8147	0.0504	0.6119
1min	0.0058	0.6619	0.0301	0.8123	0.0226	0.6104
30sec	-0.0059	0.6361	0.0210	0.8116	0.0158	0.6103
15sec	0.0063	0.6609	**0.0150**	0.8116	0.0113	0.6104
Medium Liquidity						
	Percentage Relative Bias		Relative RMSE		Relative RMAE	
Sampling frequency	$\mathcal{A}$	$\mathcal{A}^D$	$\mathcal{A}$	$\mathcal{A}^D$	$\mathcal{A}$	$\mathcal{A}^D$
1h	2.3765	2.7523	0.2453	0.8514	0.1795	0.6264
30min	1.3512	1.7998	0.1669	0.8221	0.1246	0.6155
15min	0.6757	0.8945	0.1156	0.8037	0.0869	0.6075
10min	0.4568	0.7758	0.0947	0.8015	0.0710	0.6074
5min	0.2713	0.6485	0.0665	0.7992	0.0500	0.6055
1min	0.0144	0.4765	0.0295	0.7965	0.0222	0.6045
30sec	0.0119	0.4647	0.0206	0.7961	0.0157	0.6043
15sec	-0.0248	0.4410	**0.0149**	0.7962	0.0113	0.6042
High Liquidity						
	Percentage Relative Bias		Relative RMSE		Relative RMAE	
Sampling frequency	$\mathcal{A}$	$\mathcal{A}^D$	$\mathcal{A}$	$\mathcal{A}^D$	$\mathcal{A}$	$\mathcal{A}^D$
1h	2.5093	2.9673	0.2487	0.8605	0.1804	0.6341
30min	0.9540	1.3075	0.1687	0.8297	0.1248	0.6208
15min	0.3918	0.6602	0.1171	0.8173	0.0874	0.6153
10min	0.2059	0.5948	0.0961	0.8170	0.0721	0.6146
5min	0.1975	0.5885	0.0673	0.8139	0.0505	0.6140
1min	0.0404	0.3269	0.0305	0.8087	0.0226	0.6108
30sec	0.0116	0.2842	0.0213	0.8077	0.0160	0.6106
15sec	0.0011	0.2730	**0.0149**	0.8073	0.0112	0.6105

Table 3: Illiquidity measurement. The table reports the Monte Carlo relative percentage bias, RMSE and, RMAE (all relative to $\frac{1}{\mathcal{L}}$) for several illiquidity estimators: the realized Amihud $\mathcal{A} = \frac{RPV}{v}$; the daily Amihud measure, that is, $\mathcal{A}^D = \frac{|r|}{v}$. The series $\ell(t)$ is generated according to the log Ornstein–Uhlenbeck process in (1), with parameters $\kappa_\ell = 0.05$ and $\eta_\ell = 0.1$. The smallest RMSE is in bold.

1.2 Stochastic volatility

We consider here a Monte Carlo setting where both volatility and liquidity evolve as stochastic processes. The setting of the simulations is very similar to that with constant volatility reported in Table 1, with the exception that the variances, $\sigma_j^2(t)$ $j = 1, \ldots J$, now follow the dynamics of the CIR process, that is, $d\sigma_j^2(t) = \kappa_\sigma(\sigma^2(t) - \sigma_0^2)dt + \eta_\sigma \sigma_j(t) dW_{\sigma,j}(t)$ with parameters $\kappa_\sigma = 0.05$, $\sigma_0^2 = 6$, and $\eta_\sigma = 0.05$.[1] In the various settings explored below, we change the liquidity and volatility coefficients, so to illustrate the properties of the realized Amihud to vary over time.

Furthermore, we also consider an alternative low-frequency version of the daily Amihud, that is the *high-low Amihud*. We obtain it by exploiting the high-low price range as a proxy of volatility, see Parkinson (1980), among others. In particular, the high-low Amihud is defined as $\mathcal{A}^{HL} = \frac{range}{v}$, where $range = \sqrt{\frac{1}{4\log(2)}(p^H - p^L)^2}$ with p^H and p^L being the daily high and low log-prices on a given unit interval (a day in this case).

1.2.1 Baseline Setting

Table 4 reports relative bias and RMSE for the realized Amihud, the HL Amihud and daily Amihud. The table also reports relative bias and RMSE of two new estimators, based on the inverse of the daily aggregates of two spot Amivest measures: the *smoothed Amivest*, $\mathcal{A}_s^{-1}(\tau)$ (based on a two-sided window around τ), and the *filtered Amivest*, $\mathcal{A}_f^{-1}(\tau)$ (which only uses observations in a window before τ). In both cases, the bandwidth (i.e. the length of the window for the spot estimators) is one hour. For all the estimators, the target quantity is the daily integrated illiquidity, that is $\frac{1}{\mathcal{L}}$. For all liquidity levels, the estimator with the lowest RMSE is $\overline{\mathcal{A}_s}$, that is the inverse of the daily average of the smoothed Amivest computed with returns and volume sampled at 15-second frequency. Interestingly, the realized Amihud, $\mathcal{A}$, although not being theoretically robust to stochastic volatility, displays levels of RMSE very close to those of $\overline{\mathcal{A}_s}$. This is the consequence of the fact that empirically the amount of intradaily volatility of volatility is not particularly pronounced, so that the integral $\int_0^1 \ell(s)\bar{\sigma}(s)ds$ that arises in the limit of trading volume for $I \to \infty$ is empirically very close to the product of integrals $\int_0^1 \ell(s)ds \int_0^1 \bar{\sigma}(s)ds$. Instead, the high-low Amihud and the daily Amihud are much less efficient than the realized Amihud in measuring daily illiquidity.

[1] The chosen level of σ_0^2 corresponds to a level of volatility of daily log-returns of 2.5%, a somewhat larger value of volatility than the empirical counterpart. This is done to highlight the ability of the the realized Amihud, and its spot counterparts, to extract the illiquidity signal even in settings characterized by high volatility.

Low Liquidity

Sampling frequency	Percentage Relative Bias					Relative RMSE				
	$\overline{\mathcal{A}_s}$	$\overline{\mathcal{A}_f}$	$\mathcal{A}$	$\mathcal{A}^{HL}$	$\mathcal{A}^D$	$\overline{\mathcal{A}_s}$	$\overline{\mathcal{A}_f}$	$\mathcal{A}$	$\mathcal{A}^{HL}$	$\mathcal{A}^D$
15min	-10.1547	-13.4362	0.7472	-3.4042	4.1120	0.2210	0.2596	0.1794	0.4618	1.2736
10min	-6.6812	-7.9857	0.7285	-3.4042	4.1120	0.1596	0.1766	0.1447	0.4618	1.2736
5min	-3.7582	-4.0519	0.1472	-3.4042	4.1120	0.1066	0.1118	0.0978	0.4618	1.2736
1min	-0.9260	-0.8705	0.0274	-3.4042	4.1120	0.0426	0.0448	0.0446	0.4618	1.2736
30sec	-0.4573	-0.4119	0.0798	-3.4042	4.1120	0.0290	0.0334	0.0299	0.4618	1.2736
15sec	-0.3011	-0.2649	0.0422	-3.4042	4.1120	**0.0221**	0.0292	0.0226	0.4618	1.2736

Medium Liquidity

Sampling frequency	Percentage Relative Bias					Relative RMSE				
	$\overline{\mathcal{A}_s}$	$\overline{\mathcal{A}_f}$	$\mathcal{A}$	$\mathcal{A}^{HL}$	$\mathcal{A}^D$	$\overline{\mathcal{A}_s}$	$\overline{\mathcal{A}_f}$	$\mathcal{A}$	$\mathcal{A}^{HL}$	$\mathcal{A}^D$
15min	-11.2163	-14.6809	0.1810	-3.6646	-3.4094	0.3924	0.4746	0.2240	0.6180	1.9773
10min	-6.6702	-8.1643	0.8248	-3.6646	-3.4094	0.2236	0.2596	0.1442	0.6180	1.9773
5min	-3.9566	-4.3750	-0.1258	-3.6646	-3.4094	0.1344	0.1381	0.0946	0.6180	1.9773
1min	-0.8942	-0.9205	0.0391	-3.6646	-3.4094	0.0551	0.0496	0.0638	0.6180	1.9773
30sec	-0.6679	-0.6790	-0.2349	-3.6646	-3.4094	0.0642	0.0716	0.0759	0.6180	1.9773
15sec	-0.3623	-0.3806	-0.0009	-3.6646	-3.4094	**0.0280**	0.0449	0.0358	0.6180	1.9773

High Liquidity

Sampling frequency	Percentage Relative Bias					Relative RMSE				
	$\overline{\mathcal{A}_s}$	$\overline{\mathcal{A}_f}$	$\mathcal{A}$	$\mathcal{A}^{HL}$	$\mathcal{A}^D$	$\overline{\mathcal{A}_s}$	$\overline{\mathcal{A}_f}$	$\mathcal{A}$	$\mathcal{A}^{HL}$	$\mathcal{A}^D$
15min	-10.9951	-14.6120	0.1625	-4.2758	-2.8638	0.3674	0.4313	0.2040	0.4882	1.3056
10min	-7.0540	-8.5025	0.5101	-4.2758	-2.8638	0.2116	0.2264	0.1715	0.4882	1.3056
5min	-3.8084	-4.1203	0.0517	-4.2758	-2.8638	0.1283	0.1316	0.1108	0.4882	1.3056
1min	-0.7831	-0.7803	0.2180	-4.2758	-2.8638	0.0566	0.0550	0.0519	0.4882	1.3056
30sec	-0.3909	-0.3945	0.1734	-4.2758	-2.8638	0.0309	0.0407	0.0322	0.4882	1.3056
15sec	-0.2582	-0.2513	0.0588	-4.2758	-2.8638	**0.0210**	0.0343	0.0237	0.4882	1.3056

Table 4: Integrated spot illiquidity. The table reports the Monte Carlo relative percentage bias and RMSE (both relative to $\frac{1}{\mathcal{L}}$) for several illiquidity estimators: the smoothed integrated illiquidity, denoted as $\overline{\mathcal{A}_s} = \left(\frac{1}{I}\sum_{i=1}^{I}\mathcal{A}_s^{-1}(\tau_i)\right)^{-1}$, where $\mathcal{A}_s^{-1}(\tau_i)$ is the spot Amivest based on a (equally weighted) two-sided kernel function; the filtered integrated illiquidity, denoted as $\overline{\mathcal{A}_f} = \left(\frac{1}{I}\sum_{i=1}^{I}\mathcal{A}_f^{-1}(\tau_i)\right)^{-1}$, where $\mathcal{A}_f^{-1}(\tau_i)$ is the spot Amivest based on an (equally weighted) backward kernel function; the realized Amihud $\mathcal{A} = \frac{RPV}{v}$; the daily Amihud measure, that is, $\mathcal{A}^D = \frac{|r|}{v}$; the high-low Amihud, $\mathcal{A}^{HL} = \frac{range}{v}$, where *range* is scaled by $\sqrt{2/\pi}$ to be comparable with the RPV. The series $\ell(t)$ is generated according to the log Ornstein–Uhlenbeck process in (1), with parameters $\kappa_\ell = 0.1$ and $\eta_\ell = 0.6$. The variances evolve following the dynamics of the CIR process, that is, $d\sigma_j^2(t) = \kappa_\sigma(\sigma^2(t) - \sigma_0^2)dt + \eta_\sigma\sigma(t)dW_{\sigma,j}(t)$ with the parameters $\kappa_\sigma = 0.05$, $\sigma_0^2 = 6$, $\eta_\sigma = 0.05$. The spot Amivest uses a bandwidth length of one hour. The smallest RMSE is in bold.

1.2.2 Setting 1

Spot liquidity, $\ell(t)$, evolves according to the following Ornstein–Uhlenbeck process

$$d\log\ell(t) = 0.2(\log\ell(t) - \ell_0)dt + 0.7dW(t), \qquad t > 0, \tag{2}$$

while the variances (on the scale of percentage returns) evolve following the dynamics of the CIR process

$$d\sigma_j^2(t) = 0.05\sigma(\sigma^2(t) - 6)dt + 0.05\sigma(t)dW_{\sigma,j}(t).$$

Low Liquidity										
	Percentage Relative Bias					Relative RMSE				
Sampling frequency	$\overline{\mathcal{A}_s}$	$\overline{\mathcal{A}_f}$	$\mathcal{A}$	$\mathcal{A}^{HL}$	$\mathcal{A}^D$	$\overline{\mathcal{A}_s}$	$\overline{\mathcal{A}_f}$	$\mathcal{A}$	$\mathcal{A}^{HL}$	$\mathcal{A}^D$
15min	-10.3690	-14.0067	0.9407	-0.8847	5.0471	0.2993	0.4027	0.1952	0.5455	1.3514
10min	-6.7148	-8.1868	0.6604	-0.8847	5.0471	0.1972	0.2212	0.1627	0.5455	1.3514
5min	-3.4769	-3.9317	0.5177	-0.8847	5.0471	0.1204	0.1273	0.1081	0.5455	1.3514
1min	-0.8901	-0.9487	0.1791	-0.8847	5.0471	0.0521	0.0567	0.0531	0.5455	1.3514
30sec	-0.7221	-0.7707	-0.1839	-0.8847	5.0471	0.0412	0.0469	0.0406	0.5455	1.3514
15sec	-0.4976	-0.5575	-0.1886	-0.8847	5.0471	0.0288	0.0405	**0.0287**	0.5455	1.3514
Medium Liquidity										
	Percentage Relative Bias					Relative RMSE				
Sampling frequency	$\overline{\mathcal{A}_s}$	$\overline{\mathcal{A}_f}$	$\mathcal{A}$	$\mathcal{A}^{HL}$	$\mathcal{A}^D$	$\overline{\mathcal{A}_s}$	$\overline{\mathcal{A}_f}$	$\mathcal{A}$	$\mathcal{A}^{HL}$	$\mathcal{A}^D$
15min	-11.4926	-14.9020	-0.9072	-6.1235	1.1195	0.3368	0.4117	0.2414	0.6821	1.5500
10min	-7.5927	-9.0495	0.2383	-6.1235	1.1195	0.2809	0.3142	0.1872	0.6821	1.5500
5min	-4.2517	-4.5411	-0.4191	-6.1235	1.1195	0.1424	0.1501	0.1143	0.6821	1.5500
1min	-1.1461	-1.1875	-0.2050	-6.1235	1.1195	0.0716	0.0807	0.0676	0.6821	1.5500
30sec	-0.6679	-0.7235	-0.1307	-6.1235	1.1195	0.0356	0.0529	0.0328	0.6821	1.5500
15sec	-0.3706	-0.4287	-0.0016	-6.1235	1.1195	0.0237	0.0404	**0.0219**	0.6821	1.5500
High Liquidity										
	Percentage Relative Bias					Relative RMSE				
Sampling frequency	$\overline{\mathcal{A}_s}$	$\overline{\mathcal{A}_f}$	$\mathcal{A}$	$\mathcal{A}^{HL}$	$\mathcal{A}^D$	$\overline{\mathcal{A}_s}$	$\overline{\mathcal{A}_f}$	$\mathcal{A}$	$\mathcal{A}^{HL}$	$\mathcal{A}^D$
15min	-10.5214	-14.0662	0.5619	-4.1779	-1.6551	0.2885	0.3373	0.1813	0.4522	1.1350
10min	-6.8335	-8.2686	0.7493	-4.1779	-1.6551	0.1813	0.1931	0.1725	0.4522	1.1350
5min	-3.7256	-4.0240	0.1943	-4.1779	-1.6551	0.1123	0.1160	0.1036	0.4522	1.1350
1min	-0.7930	-0.8017	0.2074	-4.1779	-1.6551	0.0495	0.0512	0.0468	0.4522	1.1350
30sec	-0.4416	-0.4553	0.1335	-4.1779	-1.6551	0.0295	0.0376	0.0297	0.4522	1.1350
15sec	-0.3036	-0.3059	0.0559	-4.1779	-1.6551	**0.0202**	0.0320	0.0231	0.4522	1.1350

Table 5: Integrated spot illiquidity. Integrated spot illiquidity. The table reports the Monte Carlo relative percentage bias and RMSE (both relative to $\frac{1}{\mathcal{L}}$) for several illiquidity estimators: the smoothed integrated illiquidity, denoted as $\overline{\mathcal{A}_s} = \left(\frac{1}{I}\sum_{i=1}^{I}\mathcal{A}_s^{-1}(\tau_i)\right)^{-1}$, where $\mathcal{A}_s^{-1}(\tau_i)$ is the spot Amivest based on a (equally weighted) two-sided kernel function; the filtered integrated illiquidity, denoted as $\overline{\mathcal{A}_f} = \left(\frac{1}{I}\sum_{i=1}^{I}\mathcal{A}_f^{-1}(\tau_i)\right)^{-1}$, where $\mathcal{A}_f^{-1}(\tau_i)$ is the spot Amivest based on an (equally weighted) backward kernel function; the realized Amihud $\mathcal{A} = \frac{RPV}{v}$; the daily Amihud measure, that is, $\mathcal{A}^D = \frac{|r|}{v}$; the high-low Amihud, $\mathcal{A}^{HL} = \frac{range}{v}$, where *range* is scaled by $\sqrt{2/\pi}$ to be comparable with the RPV. The series $\ell(t)$ is generated according to the log Ornstein–Uhlenbeck process in (1), with parameters $\kappa_\ell = 0.2$ and $\eta_\ell = 0.7$. The variances evolve following the dynamics of the CIR process, that is, $d\sigma_j^2(t) = \kappa_\sigma(\sigma^2(t) - \sigma_0^2)dt + \eta_\sigma\sigma(t)dW_{\sigma,j}(t)$ with the parameters $\kappa_\sigma = 0.05$, $\sigma_0^2 = 6$, $\eta_\sigma = 0.05$. The spot Amivest uses a bandwidth length of one hour. The smallest RMSE is in bold.

1.2.3 Setting 2

Spot liquidity, $\ell(t)$, evolves according to the following Ornstein–Uhlenbeck process

$$d \log \ell(t) = 0.3(\log \ell(t) - \ell_0)dt + 0.8dW(t), \qquad t > 0, \tag{3}$$

while the variances (on the scale of percentage returns) evolve following the dynamics of the CIR process

$$d\sigma_j^2(t) = 0.05\sigma(\sigma^2(t) - 6)dt + 0.05\sigma(t)dW_{\sigma,j}(t).$$

Low Liquidity										
	Percentage Relative Bias					Relative RMSE				
Sampling frequency	$\overline{\mathcal{A}_s}$	$\overline{\mathcal{A}_f}$	$\mathcal{A}$	$\mathcal{A}^{HL}$	$\mathcal{A}^D$	$\overline{\mathcal{A}_s}$	$\overline{\mathcal{A}_f}$	$\mathcal{A}$	$\mathcal{A}^{HL}$	$\mathcal{A}^D$
15min	-10.9543	-14.3990	0.0028	-5.2463	-3.7320	0.2620	0.3100	0.1600	0.3980	0.9806
10min	-8.0131	-9.5391	-0.1452	-5.2463	-3.7320	0.1995	0.2245	0.1251	0.3980	0.9806
5min	-4.4389	-4.8404	-0.3232	-5.2463	-3.7320	0.1192	0.1275	0.0908	0.3980	0.9806
1min	-1.2381	-1.2955	-0.2103	-5.2463	-3.7320	0.0514	0.0530	0.0463	0.3980	0.9806
30sec	-0.7859	-0.8326	-0.1550	-5.2463	-3.7320	0.0316	0.0366	0.0309	0.3980	0.9806
15sec	-0.5242	-0.5603	-0.1002	-5.2463	-3.7320	0.0269	0.0329	**0.0247**	0.3980	0.9806
Medium Liquidity										
	Percentage Relative Bias					Relative RMSE				
Sampling frequency	$\overline{\mathcal{A}_s}$	$\overline{\mathcal{A}_f}$	$\mathcal{A}$	$\mathcal{A}^{HL}$	$\mathcal{A}^D$	$\overline{\mathcal{A}_s}$	$\overline{\mathcal{A}_f}$	$\mathcal{A}$	$\mathcal{A}^{HL}$	$\mathcal{A}^D$
15min	-11.0170	-14.4757	0.3255	-3.5767	-5.2678	0.2684	0.3229	0.1771	0.4552	1.4657
10min	-6.7394	-8.2255	0.9990	-3.5767	-5.2678	0.1755	0.1890	0.1361	0.4552	1.4657
5min	-4.0039	-4.4114	0.0608	-3.5767	-5.2678	0.1152	0.1164	0.0845	0.4552	1.4657
1min	-0.9261	-0.9679	0.1351	-3.5767	-5.2678	0.0475	0.0461	0.0550	0.4552	1.4657
30sec	-0.6351	-0.6782	-0.0201	-3.5767	-5.2678	0.0353	0.0431	0.0431	0.4552	1.4657
15sec	-0.4573	-0.4994	0.0249	-3.5767	-5.2678	**0.0257**	0.0455	0.0300	0.4552	1.4657
High Liquidity										
	Percentage Relative Bias					Relative RMSE				
Sampling frequency	$\overline{\mathcal{A}_s}$	$\overline{\mathcal{A}_f}$	$\mathcal{A}$	$\mathcal{A}^{HL}$	$\mathcal{A}^D$	$\overline{\mathcal{A}_s}$	$\overline{\mathcal{A}_f}$	$\mathcal{A}$	$\mathcal{A}^{HL}$	$\mathcal{A}^D$
15min	-10.5643	-13.7643	0.4408	-4.5164	1.2396	0.2107	0.2460	0.1619	0.4386	1.0868
10min	-7.0428	-8.2826	0.4448	-4.5164	1.2396	0.1556	0.1731	0.1362	0.4386	1.0868
5min	-4.0531	-4.2903	-0.0521	-4.5164	1.2396	0.1062	0.1118	0.0929	0.4386	1.0868
1min	-1.0248	-0.9458	0.0018	-4.5164	1.2396	0.0398	0.0451	0.0398	0.4386	1.0868
30sec	-0.5306	-0.4602	0.0921	-4.5164	1.2396	0.0261	0.0348	0.0268	0.4386	1.0868
15sec	-0.4022	-0.3415	0.0218	-4.5164	1.2396	**0.0196**	0.0309	0.0201	0.4386	1.0868

Table 6: Integrated spot illiquidity. The table reports the Monte Carlo relative percentage bias and RMSE (both relative to $\frac{1}{\mathcal{L}}$) for several illiquidity estimators: the smoothed integrated illiquidity, denoted as $\overline{\mathcal{A}_s} = \left(\frac{1}{I}\sum_{i=1}^{I} \mathcal{A}_s^{-1}(\tau_i)\right)^{-1}$, where $\mathcal{A}_s^{-1}(\tau_i)$ is the spot Amivest based on a (equally weighted) two-sided kernel function; the filtered integrated illiquidity, denoted as $\overline{\mathcal{A}_f} = \left(\frac{1}{I}\sum_{i=1}^{I} \mathcal{A}_f^{-1}(\tau_i)\right)^{-1}$, where $\mathcal{A}_f^{-1}(\tau_i)$ is the spot Amivest based on an (equally weighted) backward kernel function; the realized Amihud $\mathcal{A} = \frac{RPV}{v}$; the daily Amihud measure, that is, $\mathcal{A}^D = \frac{|r|}{v}$; the high-low Amihud, $\mathcal{A}^{HL} = \frac{range}{v}$, where *range* is scaled by $\sqrt{2/\pi}$ to be comparable with the RPV. The series $\ell(t)$ is generated according to the log Ornstein–Uhlenbeck process in (1), with parameters $\kappa_\ell = 0.3$ and $\eta_\ell = 0.8$. The variances evolve following the dynamics of the CIR process, that is, $d\sigma_j^2(t) = \kappa_\sigma(\sigma^2(t) - \sigma_0^2)dt + \eta_\sigma\sigma(t)dW_{\sigma,j}(t)$ with the parameters $\kappa_\sigma = 0.05$, $\sigma_0^2 = 6$, $\eta_\sigma = 0.05$. The spot Amivest uses a bandwidth length of one hour. The smallest RMSE is in bold.

1.3 Monthly Illiquidity

We also consider the measurement of illiquidity over a longer time span, that is the monthly horizon. In this case, spot liquidity, $\ell(t)$, evolves according to the following Ornstein–Uhlenbeck process

$$d \log \ell(t) = 0.5(\log \ell(t) - \ell_0)dt + 0.95dW(t), \qquad t > 0, \tag{4}$$

while the variances (on the scale of percentage returns) evolve following the dynamics of the CIR process

$$d\sigma_j^2(t) = 0.05\sigma(\sigma^2(t) - 6)dt + 0.05\sigma(t)dW_{\sigma,j}(t).$$

	Percentage Relative Bias					Relative RMSE				
Low Liquidity										
Sampling frequency	$\overline{\mathcal{A}_s}$	$\overline{\mathcal{A}_f}$	$\mathcal{A}$	$\mathcal{A}^{HL}$	$\mathcal{A}^D$	$\overline{\mathcal{A}_s}$	$\overline{\mathcal{A}_f}$	$\mathcal{A}$	$\mathcal{A}^{HL}$	$\mathcal{A}^D$
15min	-10.5724	-13.8903	0.6419	-2.7094	4.4172	0.1490	0.1925	0.0355	0.1174	0.3227
10min	-6.9913	-8.4575	0.7600	-3.1010	3.8676	0.1002	0.1194	0.0341	0.1219	0.3151
5min	-3.5485	-3.9353	0.5628	-3.0956	4.0122	0.0555	0.0603	0.0261	0.1172	0.3120
1min	-0.7657	-0.7905	0.1891	-3.3569	3.6409	0.0140	0.0146	0.0107	0.1202	0.3097
30sec	-0.4444	-0.4588	0.1246	-3.4315	3.5718	0.0091	0.0096	0.0087	0.1190	0.3074
15sec	-0.2637	-0.2764	0.1208	-3.4864	3.5201	0.0062	0.0073	**0.0056**	0.1178	0.3052
Medium Liquidity										
	Percentage Relative Bias					Relative RMSE				
Sampling frequency	$\overline{\mathcal{A}_s}$	$\overline{\mathcal{A}_f}$	$\mathcal{A}$	$\mathcal{A}^{HL}$	$\mathcal{A}^D$	$\overline{\mathcal{A}_s}$	$\overline{\mathcal{A}_f}$	$\mathcal{A}$	$\mathcal{A}^{HL}$	$\mathcal{A}^D$
15min	-10.1277	-13.4621	1.0054	-3.5146	2.0781	0.1361	0.1797	0.0483	0.1384	0.2938
10min	-6.8135	-8.2566	0.9884	-3.5146	2.0781	0.0953	0.1140	0.0348	0.1384	0.2938
5min	-3.3891	-3.7382	0.7197	-3.5146	2.0781	0.0509	0.0552	0.0206	0.1384	0.2938
1min	-0.7459	-0.7301	0.1677	-3.5146	2.0781	0.0153	0.0145	0.0115	0.1384	0.2938
30sec	-0.4202	-0.3958	0.1204	-3.5146	2.0781	0.0098	0.0091	0.0076	0.1384	0.2938
15sec	-0.2735	-0.2536	0.0425	-3.5146	2.0781	0.0052	0.0053	**0.0040**	0.1384	0.2938
High Liquidity										
	Percentage Relative Bias					Relative RMSE				
Sampling frequency	$\overline{\mathcal{A}_s}$	$\overline{\mathcal{A}_f}$	$\mathcal{A}$	$\mathcal{A}^{HL}$	$\mathcal{A}^D$	$\overline{\mathcal{A}_s}$	$\overline{\mathcal{A}_f}$	$\mathcal{A}$	$\mathcal{A}^{HL}$	$\mathcal{A}^D$
15min	-10.0334	-13.5023	0.8992	-4.4136	-2.7195	0.1358	0.1857	0.0435	0.1246	0.4341
10min	-7.4173	-8.8670	0.0961	-4.4136	-2.7195	0.1074	0.1283	0.0276	0.1246	0.4341
5min	-3.6598	-4.0057	0.2617	-4.4136	-2.7195	0.0545	0.0596	0.0249	0.1246	0.4341
1min	-0.9282	-0.9041	-0.0993	-4.4136	-2.7195	0.0174	0.0173	0.0101	0.1246	0.4341
30sec	-0.5329	-0.4949	-0.0802	-4.4136	-2.7195	0.0137	0.0130	0.0121	0.1246	0.4341
15sec	-0.3791	-0.3393	-0.0449	-4.4136	-2.7195	0.0109	0.0102	**0.0094**	0.1246	0.4341

Table 7: Monthly Integrated spot illiquidity. The table reports the Monte Carlo relative percentage bias and RMSE (both relative to $\frac{1}{\mathcal{L}}$) for several illiquidity estimators aggregated at a monthly level: the smoothed integrated illiquidity, denoted as $\overline{\mathcal{A}_s} = \left(\frac{1}{I}\sum_{i=1}^{I} \mathcal{A}_s^{-1}(\tau_i)\right)^{-1}$, where $\mathcal{A}_s^{-1}(\tau_i)$ is the spot Amivest based on a (equally weighted) two-sided kernel function; the filtered integrated illiquidity, denoted as $\overline{\mathcal{A}_f} = \left(\frac{1}{I}\sum_{i=1}^{I} \mathcal{A}_f^{-1}(\tau_i)\right)^{-1}$, where $\mathcal{A}_f^{-1}(\tau_i)$ is the spot Amivest based on an (equally weighted) backward kernel function; the realized Amihud $\mathcal{A} = \frac{RPV}{\mathcal{V}}$; the daily Amihud measure, that is, $\mathcal{A}^D = \frac{|r|}{\mathcal{V}}$; the high-low Amihud, $\mathcal{A}^{HL} = \frac{range}{\mathcal{V}}$, where *range* is scaled by $\sqrt{2/\pi}$ to be comparable with the RPV. The series $\ell(t)$ is generated according to the log Ornstein–Uhlenbeck process in (1), with parameters $\kappa_\ell = 0.5$ and $\eta_\ell = 0.95$. The variances evolve following the dynamics of the CIR process, that is, $d\sigma_j^2(t) = \kappa_\sigma(\sigma^2(t) - \sigma_0^2)dt + \eta_\sigma\sigma(t)dW_{\sigma,j}(t)$ with the parameters $\kappa_\sigma = 0.05$, $\sigma_0^2 = 6$, $\eta_\sigma = 0.05$. The spot Amivest uses a bandwidth length of one hour. The smallest RMSE is in bold.

1.4 Realized Amihud and Market Microstructure Noise

Low Liquidity						
	Percentage Relative Bias			Relative RMSE		
Sampling frequency	$\mathcal{A}$	$\mathcal{A}^{HL}$	$\mathcal{A}^{D}$	$\mathcal{A}$	$\mathcal{A}^{HL}$	$\mathcal{A}^{D}$
1hour	1.8020	-4.8748	-0.7818	0.2176	0.3054	0.7711
30min	1.8298	-4.8748	-0.7818	0.1569	0.3054	0.7711
15min	1.6781	-4.8748	-0.7818	0.1151	0.3054	0.7711
10min	1.7789	-4.8748	-0.7818	0.0921	0.3054	0.7711
5min	2.9765	-4.8748	-0.7818	**0.0725**	0.3054	0.7711
1min	13.3029	-4.8748	-0.7818	0.1476	0.3054	0.7711
30sec	25.1862	-4.8748	-0.7818	0.2720	0.3054	0.7711
15sec	28.4629	-4.8748	-0.7818	0.3149	0.3054	0.7711
Medium Liquidity						
	Percentage Relative Bias			Relative RMSE		
Sampling frequency	$\mathcal{A}$	$\mathcal{A}^{HL}$	$\mathcal{A}^{D}$	$\mathcal{A}$	$\mathcal{A}^{HL}$	$\mathcal{A}^{D}$
1hour	2.9646	-4.8349	-1.9522	0.2258	0.2812	0.7334
30min	1.5911	-4.8349	-1.9522	0.1587	0.2812	0.7334
15min	1.5683	-4.8349	-1.9522	0.1110	0.2812	0.7334
10min	1.8408	-4.8349	-1.9522	0.0930	0.2812	0.7334
5min	2.6054	-4.8349	-1.9522	**0.0690**	0.2812	0.7334
1min	12.0901	-4.8349	-1.9522	0.1276	0.2812	0.7334
30sec	22.9034	-4.8349	-1.9522	0.2355	0.2812	0.7334
15sec	25.5046	-4.8349	-1.9522	0.2640	0.2812	0.7334
High Liquidity						
	Percentage Relative Bias			Relative RMSE		
Sampling frequency	$\mathcal{A}$	$\mathcal{A}^{HL}$	$\mathcal{A}^{D}$	$\mathcal{A}$	$\mathcal{A}^{HL}$	$\mathcal{A}^{D}$
1hour	1.8504	-5.9370	-1.3766	0.2463	0.2818	0.7248
30min	0.9157	-5.9370	-1.3766	0.1640	0.2818	0.7248
15min	0.9431	-5.9370	-1.3766	0.1097	0.2818	0.7248
10min	1.1633	-5.9370	-1.3766	0.0892	0.2818	0.7248
5min	2.2907	-5.9370	-1.3766	**0.0676**	0.2818	0.7248
1min	8.9761	-5.9370	-1.3766	0.0964	0.2818	0.7248
30sec	16.9324	-5.9370	-1.3766	0.1736	0.2818	0.7248
15sec	17.0739	-5.9370	-1.3766	0.1764	0.2818	0.7248

Table 8: Illiquidity measurement with microstructure noise. The table reports Monte Carlo simulations for assessing the quality of illiquidity through the realized Amihud. The bid-ask spread is set at 0.15% relative to the price level. Table reports the Monte Carlo relative percentage bias and RMSE (both relative to $\frac{1}{\mathcal{L}}$) for the realized Amihud. The smallest RMSE is in bold. As a reference, we also consider the daily Amihud measure, that is, $\mathcal{A}^D = \frac{|r|}{v}$, and the high-low Amihud, $\mathcal{A}^{HL} = \frac{range}{v}$, where *range* is scaled by $\sqrt{2/\pi}$ to be comparable with the RPV.

2 Information Jumps

We explore the relationship between liquidity and volatility, focusing on the arrival of large news common to traders. Note that the increments of the reservation log-prices can be disentangled as

$$\Delta p^*_{i,j} = \phi_i + \psi_{i,j}, \quad \text{with} \quad j = 1, \ldots, J,$$

where ϕ_i represents a fundamental information component common to all traders, stemming from public information events, such as those associated with earnings press releases or central banks' announcements. This could be related to events that trigger common directional beliefs among practitioners. The term $\psi_{i,j}$ is the change in the discretized diffusive process outlined in Section 2 (equation 3) of the main document, which represents the investor's specific component of the reservation price variation. Detecting such informational events requires accurate econometric techniques and granular intraday data.

The recent advances in the literature on *jump* processes help in this analysis. Similarly to Bollerslev et al. (2018), we rely on a simple setup for the common news component, to separately identify it from the component of price variation due to the disagreement among traders, which is responsible for generating the trading volume.[2] For this reason, we refer to the term ϕ_i as *information jumps*. In other words, when major news impacts the market, reservation prices all shift in the same direction, establishing a new equilibrium with increased price volatility and minimal trading volume. This causes a sharp rise in realized Amihud, which ideally should be disentangled from the baseline illiquidity associated with the trading mechanism in Section 2 (equation 1) in the main document.

We rely upon the theory of multipower variation developed in Barndorff-Nielsen and Shephard (2003, 2004, 2006) to carry out inference on information jumps in illiquidity. As in Barndorff-Nielsen and Shephard (2004) (equation 17 on page 13), we assume that ϕ_i is a compound Poisson process, namely $\phi_i = \sum_{j=1}^{\mathcal{N}_i} c_j$, where $\mathcal{N}_i$ is a simple process (e.g., a Poisson) that counts the number of jump arrivals in the interval $[i-1, i]$, and it is finite for all intervals i. The terms c_j are nonzero random variables that determine the size of the jumps. When $\mathcal{N}_i = 0$, then $\Delta p^*_{i,j}$ reduces to the stochastic volatility plus drift model, whose dynamics are described in equation 3 of Section 2 (main document). To carry out inference on jumps, we consider the multipower variation of order $1/2$, namely

$$MPV = \frac{I}{I-1} \sum_{i=2}^{I} |r_i|^{1/2} |r_{i-1}|^{1/2}. \tag{5}$$

As in Theorem 1 in Barndorff-Nielsen and Shephard (2004), MPV converges to $\mathcal{S}$, even when $\phi_i \neq 0$, i.e.,

$$p \lim_{I \to \infty} \delta^{1/2} \mu_{1/2}^{-2} MPV = \mathcal{S}, \tag{6}$$

where $\mu_{1/2} = E[|X|]^{1/2}$ is a normalizing constant. Therefore, as in Theorem 1 of Barndorff-Nielsen and Shephard (2006), we can devise the jump test statistic, $\mathcal{J}$, defined as

$$\mathcal{J} = \frac{\sqrt{\pi/2}\mu_{1/2}^2 RPV - MPV}{\widetilde{BPV}}, \tag{7}$$

where $\widetilde{BPV} = \sqrt{\xi \sum_{i=2}^{I} |r_i||r_{i-1}|}$ and $\xi = \theta(\mu_1^2 + 2\mu_{1/2}^2\mu_1 - 3\mu_{1/2}^4)/\mu_1^2)$ is a scaling constant with $\theta = 0.1032$. Under the null hypothesis that $\phi_i = 0$, $\mathcal{J} \xrightarrow{d} N(0,1)$, we can use this result for testing the presence of a significant information jump in a given day. With the goal of wiping out the impact of information jumps on $\mathcal{A}$, we can construct the *jump-robust* realized Amihud as

$$\mathcal{A}^C = \frac{RPV_C}{v}, \tag{8}$$

[2] Other studies associating large price jumps with news announcements can be found in Andersen et al. (2007), Chaboud et al. (2008), Lee (2011), Jiang et al. (2011).

where RPV_C is the jump-robust realized power variation, given by

$$RPV_C = \mathbb{I}(\mathcal{J} \leq q_{1-\alpha})RPV + \mathbb{I}(\mathcal{J} > q_{1-\alpha})\widetilde{MPV}, \tag{9}$$

where $\mathbb{I}(\cdot)$ is the indicator function, $q_{1-\alpha}$ denotes the $(1-\alpha)$-th quantile of a standard Gaussian distribution, α is the significance level of the jump test, and $\widetilde{MPV} = \sqrt{2/\pi}\mu_{1/2}^{-2}MPV$.

Monte Carlo simulations in Table 9 assess the properties of the $\mathcal{J}$-test in terms of the empirical size and power. In frictionless settings with nominal sizes of $\alpha = 5\%, 1\%, 0.5\%$, the test performs best at 15-second sampling intervals. When $\phi_i \neq 0$, the test correctly identifies jumps in over 90% of cases when sampling at high frequencies, demonstrating strong power to detect jumps. As expected, when microstructure noise is introduced—modeled as a bid-ask spread of 0.15% relative to the price level—the $\mathcal{J}$-test exhibits inflated rejection rates at very high sampling frequencies. In particular, at the 15-second frequency, size distortions become severe despite an apparent increase in statistical power. The optimal trade-off between size accuracy and detection ability is achieved at the 1-hour frequency, where the empirical size remains close to nominal levels and the test power exceeds 75%. Nevertheless, the test continues to perform reasonably well at the 5-minute frequency, offering a balanced compromise between robustness and sensitivity.

	No noise						Microstructure noise					
Low Liquidity	Power			Size			Power			Size		
	5%	1%	0.5%	5%	1%	0.5%	5%	1%	0.5%	5%	1%	0.5%
1h	79.83%	75.35%	73.80%	10.31%	4.69%	3.52%	80.99%	76.34%	74.43%	10.98%	5.08%	3.98%
30min	84.71%	80.85%	79.55%	8.48%	3.16%	2.18%	84.94%	81.39%	79.92%	10.78%	4.70%	3.32%
15min	86.97%	83.54%	82.56%	7.68%	2.51%	1.56%	88.59%	85.77%	84.44%	11.04%	4.64%	3.28%
10min	88.83%	85.83%	84.40%	6.65%	2.02%	1.29%	90.49%	87.41%	86.32%	12.26%	4.74%	3.16%
5min	90.55%	87.55%	86.48%	6.25%	1.77%	1.10%	93.07%	90.78%	89.83%	20.64%	8.82%	6.44%
1min	92.67%	90.19%	89.16%	5.63%	1.35%	0.77%	98.96%	98.22%	97.87%	97.62%	93.02%	90.92%
30sec	93.35%	90.71%	89.77%	5.72%	1.33%	0.69%	99.70%	99.45%	99.32%	100.00%	100.00%	100.00%
15sec	93.52%	91.45%	90.67%	5.44%	1.18%	0.63%	99.96%	99.96%	99.94%	100.00%	100.00%	100.00%
Medium Liquidity	Power			Size			Power			Size		
	5%	1%	0.5%	5%	1%	0.5%	5%	1%	0.5%	5%	1%	0.5%
1h	79.87%	75.46%	73.96%	10.70%	4.89%	3.69%	80.04%	75.75%	73.89%	10.96%	5.00%	3.88%
30min	85.06%	81.18%	79.60%	8.72%	3.42%	2.31%	84.32%	80.17%	78.93%	8.94%	3.50%	2.44%
15min	87.82%	84.48%	83.05%	7.07%	2.42%	1.54%	88.67%	85.07%	83.44%	8.84%	3.06%	1.90%
10min	89.16%	86.04%	84.94%	6.98%	2.29%	1.30%	89.99%	86.88%	85.93%	8.54%	2.72%	1.64%
5min	90.47%	87.56%	86.65%	6.53%	1.92%	1.05%	93.05%	90.22%	89.17%	10.76%	4.00%	2.56%
1min	92.86%	90.29%	89.55%	5.66%	1.24%	0.68%	99.27%	98.59%	98.34%	56.15%	36.61%	30.07%
30sec	93.13%	90.97%	90.05%	5.47%	1.38%	0.81%	99.70%	99.62%	99.54%	97.88%	92.80%	89.72%
15sec	93.59%	91.15%	90.48%	5.77%	1.35%	0.73%	100.00%	99.92%	99.92%	100.00%	100.00%	100.00%
High Liquidity	Power			Size			Power			Size		
	5%	1%	0.5%	5%	1%	0.5%	5%	1%	0.5%	5%	1%	0.5%
1h	80.24%	76.05%	74.22%	10.48%	5.10%	4.10%	81.21%	76.91%	75.55%	10.72%	5.16%	3.90%
30min	84.04%	80.22%	78.79%	8.53%	3.32%	2.31%	86.53%	82.76%	81.48%	10.12%	4.48%	3.22%
15min	87.96%	84.13%	82.89%	7.51%	2.54%	1.64%	89.81%	86.61%	85.37%	12.22%	4.96%	3.48%
10min	89.04%	85.32%	84.49%	6.86%	2.23%	1.43%	90.74%	87.90%	86.92%	13.52%	5.52%	3.76%
5min	90.59%	88.03%	86.67%	6.46%	1.87%	1.12%	94.07%	91.53%	90.66%	24.08%	11.30%	8.14%
1min	92.40%	90.14%	89.25%	5.67%	1.29%	0.67%	99.74%	99.27%	99.13%	97.84%	94.36%	92.30%
30sec	93.22%	91.00%	90.02%	5.45%	1.35%	0.71%	100.00%	99.94%	99.92%	100.00%	100.00%	99.98%
15sec	93.69%	91.52%	90.64%	5.35%	1.21%	0.69%	99.98%	99.98%	99.98%	100.00%	100.00%	100.00%

Table 9: Jump test: power and size. The table reports Monte Carlo simulations for the assessment of the power and size of the jump test without microstructure noise (left panel) and with microstructure noise (right panel). In the configuration with microstructure noise, the bid-ask spread is set at 0.15% relative to the price level. The empirical size and power of the jump test are computed at the 5%, 1%, and 0.5% theoretical size levels, respectively.

3 Correlations of Illiquidity Measurements

	$\mathcal{A}$	$\mathcal{A}^{\mathcal{RV}}$	$\mathcal{A}^{Spot}$	$\mathcal{A}^{BBD}$	$\mathcal{A}^{\mathcal{D}}$	λ	BAS	EC	CS	AR
$\mathcal{A}$	1	0.986	0.992	0.693	0.320	0.584	0.482	0.318	0.331	0.230
$\mathcal{A}^{\mathcal{RV}}$	0.989	1	0.974	0.690	0.312	0.560	0.476	0.312	0.304	0.220
$\mathcal{A}^{Spot}$	0.990	0.976	1	0.697	0.325	0.608	0.505	0.341	0.364	0.254
$\mathcal{A}^{BBD}$	0.660	0.655	0.666	1	0.395	0.514	0.457	0.326	0.373	0.247
$\mathcal{A}^{\mathcal{D}}$	0.263	0.253	0.274	0.325	1	0.262	0.228	0.157	0.294	0.201
λ	0.508	0.475	0.524	0.481	0.252	1	0.640	0.681	0.740	0.480
BAS	0.351	0.340	0.362	0.382	0.217	0.439	1	0.924	0.610	0.425
EC	0.160	0.152	0.169	0.232	0.145	0.535	0.876	1	0.608	0.422
CS	0.206	0.172	0.233	0.327	0.333	0.621	0.407	0.418	1	0.505
AR	0.051	0.035	0.064	0.099	0.161	0.234	0.175	0.192	0.314	1

Table 10: Correlation matrix for the daily illiquidity measures for the portfolio of the 1^{st} tercile, i.e. the average among the first 8 tickers weighted by the market capitalization. Pearson (Spearman) correlations are reported in the lower (upper) triangular portion of the table. $\mathcal{A}$ is the 1-minute realized Amihud; $\mathcal{A}^{\mathcal{RV}}$, is the realized Amihud computed with RV; $\mathcal{A}^{Spot}$ is the spot Amihud; $\mathcal{A}^{BBD}$ is the average per-dollar absolute returns of fixed-dollar volumes; $\mathcal{A}^{\mathcal{D}}$ is the daily Amihud. λ is the Kyle lambda; BAS denotes the quoted bid-ask spread; *EC* the effective cost; *CS* the Corwin–Schultz spread estimator and AR the Abdi–Ranaldo high–low spread estimator.

	$\mathcal{A}$	$\mathcal{A}^{\mathcal{RV}}$	$\mathcal{A}^{Spot}$	$\mathcal{A}^{BBD}$	$\mathcal{A}^{\mathcal{D}}$	λ	BAS	EC	CS	AR
$\mathcal{A}$	1	0.989	0.992	0.841	0.421	0.771	0.707	0.620	0.545	0.380
$\mathcal{A}^{\mathcal{RV}}$	0.988	1	0.978	0.834	0.415	0.751	0.690	0.603	0.522	0.369
$\mathcal{A}^{Spot}$	0.989	0.974	1	0.838	0.425	0.791	0.715	0.626	0.572	0.399
$\mathcal{A}^{BBD}$	0.799	0.788	0.798	1	0.467	0.740	0.677	0.599	0.582	0.390
$\mathcal{A}^{\mathcal{D}}$	0.354	0.342	0.358	0.397	1	0.419	0.370	0.332	0.417	0.295
λ	0.700	0.664	0.718	0.681	0.369	1	0.771	0.784	0.788	0.517
BAS	0.592	0.566	0.588	0.587	0.336	0.632	1	0.949	0.743	0.489
EC	0.464	0.438	0.456	0.465	0.281	0.649	0.917	1	0.719	0.456
CS	0.365	0.333	0.389	0.468	0.395	0.661	0.571	0.542	1	0.549
AR	0.163	0.150	0.178	0.198	0.218	0.287	0.262	0.244	0.356	1

Table 11: Correlation matrix for the daily illiquidity measures for the portfolio of the 2^{nd} tercile, i.e. the average among the second 9 tickers weighted by the market capitalization. Pearson (Spearman) correlations are reported in the lower (upper) triangular portion of the table. $\mathcal{A}$ is the 1-minute realized Amihud; $\mathcal{A}^{\mathcal{RV}}$, is the realized Amihud computed with RV; $\mathcal{A}^{Spot}$ is the spot Amihud; $\mathcal{A}^{BBD}$ is the average per-dollar absolute returns of fixed-dollar volumes; $\mathcal{A}^{\mathcal{D}}$ is the daily Amihud. λ is the Kyle lambda; BAS denotes the quoted bid-ask spread; *EC* the effective cost; *CS* the Corwin–Schultz spread estimator and AR the Abdi–Ranaldo high–low spread estimator.

	$\mathcal{A}$	$\mathcal{A}^{\mathcal{RV}}$	$\mathcal{A}^{Spot}$	$\mathcal{A}^{BBD}$	$\mathcal{A}^{\mathcal{D}}$	λ	BAS	EC	CS	AR
$\mathcal{A}$	1	0.990	0.994	0.873	0.437	0.624	0.709	0.393	0.492	0.304
$\mathcal{A}^{\mathcal{RV}}$	0.991	1	0.981	0.871	0.432	0.597	0.690	0.368	0.469	0.293
$\mathcal{A}^{Spot}$	0.993	0.982	1	0.874	0.445	0.650	0.732	0.416	0.523	0.327
$\mathcal{A}^{BBD}$	0.854	0.849	0.853	1	0.475	0.602	0.672	0.352	0.518	0.327
$\mathcal{A}^{\mathcal{D}}$	0.416	0.410	0.421	0.457	1	0.318	0.352	0.170	0.363	0.253
λ	0.572	0.539	0.590	0.555	0.283	1	0.774	0.823	0.726	0.465
BAS	0.731	0.712	0.743	0.687	0.400	0.642	1	0.811	0.770	0.461
EC	0.291	0.266	0.299	0.253	0.119	0.763	0.629	1	0.669	0.390
CS	0.375	0.350	0.395	0.427	0.357	0.569	0.579	0.459	1	0.533
AR	0.144	0.132	0.156	0.171	0.174	0.229	0.243	0.194	0.315	1

Table 12: Correlation matrix for the daily illiquidity measures for the portfolio of the 3^{rd} tercile, i.e. the average among the last 8 tickers weighted by the market capitalization. Pearson (Spearman) correlations are reported in the lower (upper) triangular portion of the table. $\mathcal{A}$ is the 1-minute realized Amihud; $\mathcal{A}^{\mathcal{RV}}$, is the realized Amihud computed with RV; $\mathcal{A}^{Spot}$ is the spot Amihud; $\mathcal{A}^{BBD}$ is the average per-dollar absolute returns of fixed-dollar volumes; $\mathcal{A}^{\mathcal{D}}$ is the daily Amihud. λ is the Kyle lambda; BAS denotes the quoted bid-ask spread; *EC* the effective cost; *CS* the Corwin–Schultz spread estimator and AR the Abdi–Ranaldo high–low spread estimator.

	$\mathcal{A}$	$\mathcal{A}^{\mathcal{RV}}$	$\mathcal{A}^{Spot}$	$\mathcal{A}^{BBD}$	$\mathcal{A}^{\mathcal{D}}$
$\mathcal{A}$	1	0.987	0.986	0.356	0.484
$\mathcal{A}^{\mathcal{RV}}$	0.991	1	0.972	0.339	0.473
$\mathcal{A}^{Spot}$	0.991	0.980	1	0.336	0.488
$\mathcal{A}^{BBD}$	0.428	0.413	0.417	1	0.270
$\mathcal{A}^{\mathcal{D}}$	0.523	0.510	0.529	0.275	1

Table 13: Correlation matrix for the daily illiquidity measures for the portfolio of the low capitalized assets, i.e. the average among the last 8 tickers of the Standard and Poor's 500 index weighted by the market capitalization. Pearson (Spearman) correlations are reported in the lower (upper) triangular portion of the table. $\mathcal{A}$ is the 1-minute realized Amihud; $\mathcal{A}^{\mathcal{RV}}$, is the realized Amihud computed with RV; $\mathcal{A}^{Spot}$ is the spot Amihud; $\mathcal{A}^{BBD}$ is the average per-dollar absolute returns of fixed-dollar volumes; $\mathcal{A}^{\mathcal{D}}$ is the daily Amihud.

4 Analysis on Excess Returns

In this section, we report the figure corresponding to the excess-return analysis presented in Table 6 of Section 3.3 of the main paper, providing additional visual evidence to support the results discussed therein. Figure 1 report the estimates of β_2 for different aggregation frequencies, using the realized (Panel a) and the classic Amihud (Panel b) measures, respectively. From these figures, it is clear that the unexpected component of illiquidity ($\hat{\epsilon}_t$) is negatively related to excess returns, when considering the realized Amihud. In contrast, when using the original Amihud measure the unexpected component of illiquidity impacts stock returns with a statistically significant negative effect only for horizon $K \geq 5$. These results suggest that hypotheses (i) and (ii) are more likely to hold when using the more accurate realized Amihud measure.

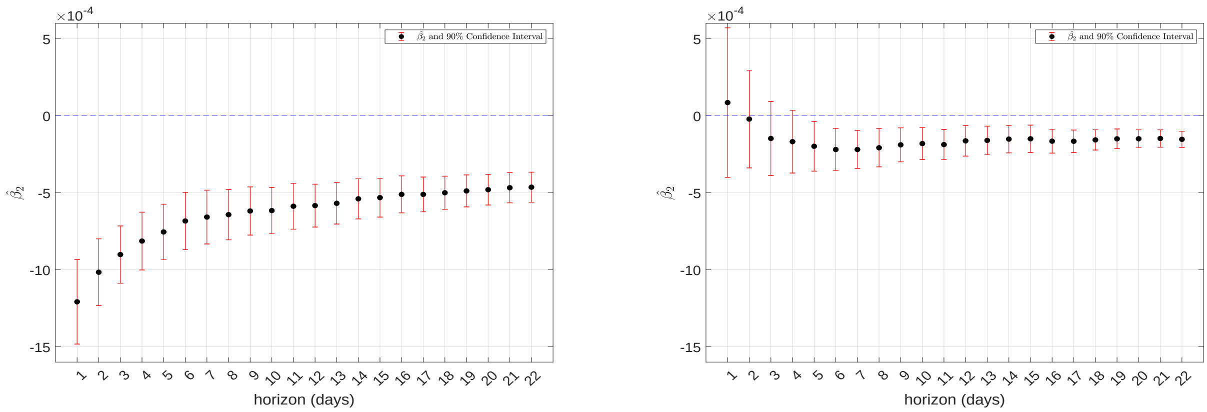

(a) Realized Amihud - Unexpected

(b) Daily Amihud - Unexpected

Figure 1: Illiqudity Shocks and Excess Returns. Panels a) and b) report the estimates of β_2 (black dots) in equation 17 of the main document obtained with the realized and daily Amihud, respectively, with a 90% interval (red bars) as a function of the aggregation horizon, $K = 1 \ldots 22$, that is reported on the x-axis.

low-cap portfolio	Daily $\mathcal{A}$	Daily $\mathcal{A}^{\mathcal{D}}$	Weekly $\mathcal{A}$	Weekly $\mathcal{A}^{\mathcal{D}}$	Monthly $\mathcal{A}$	Monthly $\mathcal{A}^{\mathcal{D}}$
Intercepet	0.0641	0.1294	0.0179	0.0283	-0.0003	-0.0065
	(0.0898)	(0.1649)	(0.0544)	(0.0455)	(0.0522)	(0.0451)
Expected Illiquidity ($\hat{\mu}_t$)	-0.0406	-0.1063	0.0054	-0.0049	0.0230	0.0295
	(0.0932)	(0.1696)	(0.0568)	(0.0482)	(0.0540)	(0.0465)
Unexpected Illiquidity ($\hat{\epsilon}_t$)	-0.0196	0.0048	-0.0395^b	-0.0134	-0.0286^a	-0.0154^a
	(0.0238)	(0.0209)	(0.0156)	(0.0099)	(0.0079)	(0.0044)
			Diagnostic			
R^2	0.0069	0.0064	0.0442	0.0289	0.0711	0.0409
R^2 adj.	0.0053	0.0048	0.0426	0.0273	0.0696	0.0393
F-stat (pvalue)	0.0116	0.0274	0.0000	0.0000	0.0000	0.0000

Table 14: Analysis regressing stock market excess returns on illiquidity decomposed into expected and unexpected components, as estimated from an AR(1) model for the portfolio of the low capitalized assets, i.e. the average among the last 8 tickers of the Standard and Poor's 500 index weighted by the market capitalization. Coefficients and Newey and West (1987) robust standard errors (in parenthesis) are scaled by factor of 100. Superscript a, b and c denote the 1%, 5%, and 10% levels of significance, respectively.

References

Andersen, T. G., Bollerslev, T., Diebold, F. X., and Vega, C. (2007). Real-time price discovery in global stock, bond and foreign exchange markets. *Journal of International Economics*, 73(2):251–277.

Barndorff-Nielsen, O. E. and Shephard, N. (2003). Realized power variation and stochastic volatility models. *Bernoulli*, 9(2):243–265.

Barndorff-Nielsen, O. E. and Shephard, N. (2004). Power and bipower variation with stochastic volatility and jumps. *Journal of Financial Econometrics*, 2(1):1–37.

Barndorff-Nielsen, O. E. and Shephard, N. (2006). Econometrics of testing for jumps in financial economics using bipower variation. *Journal of Financial Econometrics*, 4(1):1–30.

Bollerslev, T., Li, J., Xue, Y., et al. (2018). Volume, volatility and public news announcements. *The Review of Economic Studies*, 85(4):2005–2041.

Chaboud, A. P., Chernenko, S. V., and Wright, J. H. (2008). Trading activity and macroeconomic announcements in high-frequency exchange rate data. *Journal of the European Economic Association*, 6(2-3):589–596.

Comte, F. and Renault, E. (1998). Long memory in continuous-time stochastic volatility models. *Mathematical Finance*, 8(4):291–323.

Corsi, F. and Renò, R. (2012). Discrete-time volatility forecasting with persistent leverage effect and the link with continuous-time volatility modeling. *Journal of Business & Economic Statistics*, 30(3):368–380.

Jiang, G. J., Lo, I., and Verdelhan, A. (2011). Information shocks, liquidity shocks, jumps, and price discovery: Evidence from the US treasury market. *Journal of Financial and Quantitative Analysis*, 46(2):527–551.

Lee, S. S. (2011). Jumps and information flow in financial markets. *The Review of Financial Studies*, 25(2):439–479.

Melino, A. and Turnbull, S. M. (1990). Pricing foreign currency options with stochastic volatility. *Journal of econometrics*, 45(1-2):239–265.

Newey, W. K. and West, K. D. (1987). A simple, positive semi-definite, heteroskedasticity and autocorrelation consistent covariance matrix. *Econometrica*, 55:703–708.

Parkinson, M. (1980). The extreme value method for estimating the variance of the rate of return. *Journal of Business*, 53:61–65.

Rossi, E. and Santucci de Magistris, P. (2018). Indirect inference with time series observed with error. *Journal of Applied Econometrics*, 33(6):874–897.